Optical fingerprint of bright and dark localized excitonic states in atomically thin 2D materials

Maja Feierabend, Samuel Brem and Ermin Malic
Chalmers University of Technology, Department of Physics, 412 96 Gothenburg, Sweden

-SUPPLEMENTARY MATERIAL -

EQUATIONS OF MOTION IN EXCITONIC BASIS AND CAPTURE RATES

The dynamics of exciton densities appearing in the main text follow from the TMD Bloch equations [1, 2] and can be written in its general form :

$$\dot{N}^{\mu}_{\mathbf{Q}} = \sum_{\nu,\mathbf{Q}'} \Gamma^{\nu\mu,\text{in}}_{\mathbf{Q}'\mathbf{Q}} |P^{\nu}_{\mathbf{Q}'}|^2 \delta_{\mathbf{Q}',\mathbf{0}} - \Gamma^{\mu}_{\text{rad}} N^{\mu}_{\mathbf{Q}} \delta_{\mathbf{Q},\mathbf{0}} + \sum_{\nu,\mathbf{Q}'} \left(\Gamma^{\nu\mu,\text{in}}_{\mathbf{Q}'\mathbf{Q}} N^{\nu}_{\mathbf{Q}'} - \Gamma^{\mu\nu,\text{out}}_{\mathbf{Q}\mathbf{Q}'} N^{\mu}_{\mathbf{Q}} \right) \tag{S1}$$

The dephasing of the coherence $P^{\nu}_{\mathbf{Q}'}$ leads to the formation of incoherent excitons. The first contribution proportional to $\propto |P^2|$ is the driving term for the considered dynamics of excitons. The incoherent excitons can decay radiatively with the rate $\Gamma^{\mu}_{\text{rad}}$ (second contribution in Eq. S1), as long as they are located within the light cone with $\mathbf{Q} \approx 0$. This is valid for both free and localized KK excitons. Moreover, the incoherent excitons thermalize towards a thermal Bose distribution through exciton-phonon scattering (third contribution in Eq. S1). This is determined by out-scattering rates $\Gamma^{\mu\nu,\text{out}}_{\mathbf{Q}\mathbf{Q}'}$ describing phonon-driven scattering from the state $(\mu, \mathbf{Q})$ to the state $(\nu, \mathbf{Q}')$ and in-scattering rates $\Gamma^{\nu\mu,\text{in}}_{\mathbf{Q}'\mathbf{Q}}$ describing the reverse process. Transforming now in the localized exciton basis, we find for the dynamics of localized excitons:

$$\dot{N}^{\mu m} = \sum_{\nu n} \Gamma^{\nu n \mu m} |P^{\nu n}|^2 - \Gamma^{\mu}_{\text{rad}} |\chi^{\mu m}_{Q=0}|^2 N^{\mu m} + \sum_{\nu n} \left(\Gamma^{\nu n \mu m} N^{\nu n} - \Gamma^{\mu m \nu n} N^{\mu m} \right) \tag{S2}$$

with exciton-phonon scattering rate [2] in localized exciton basis

$$\Gamma^{\nu n \mu m} = \frac{2\pi}{\hbar} \sum_{\alpha Q'} |D^{\nu n \mu m}_{\alpha Q'}|^2 \left(\frac{1}{2} \mp \frac{1}{2} + n^{\text{phon}}_{\alpha Q'} \right) \delta(\varepsilon^{\mu m} - \varepsilon^{\nu n} \pm \Omega^{\alpha}_{Q'}) \quad . \tag{S3}$$

where $D^{\nu n \mu m}_{\alpha Q'}$ corresponds to the exciton-phonon matrix elements ,$n^{\text{phon}}_{\alpha Q}$ describes the phonon occupation, Ω^{α}_{Q} denoting the energy of the involved phonon, and $\varepsilon^{\mu m}$corresponding to the exciton energy of the involved states. The delta distribution in Eq. (S3) assures energy conservation between initial and final exciton state under emission/absorption of phonons.

The appearing exciton-phonon matrix elements read

$$D^{\nu n \mu m}_{\alpha Q} = \sum_{q Q'} \chi^{\nu n *}_{Q} \varphi^{\nu *}_{q} g^{cc}_{Q'\alpha} \varphi^{\mu}_{q+\beta Q'} \chi^{\mu m}_{Q+Q'} \tag{S4}$$

including both free φ and localized χ wavefunctions and the electron-phonon coupling elements $g^{cc}_{Q\alpha}$ [3] . Depending on initial and final state we can distinguish three processes: (i) Free $\rightarrow$ Free described by $\Gamma^{\nu\mu,\text{phon}}_{\mathbf{Q}'\mathbf{Q}}$, (ii) Loc $\rightarrow$ Loc described by $\Gamma^{\nu n \mu m,\text{loc}}$, and (iii) Free $\rightarrow$ Loc (Loc $\rightarrow$ Free) described by $\Gamma^{\nu F \mu m,\text{capt}}$ ($\Gamma^{\mu m \nu F,\text{esc}}$). Scattering between free exciton states includes both intra- and inter-valley scattering. Scattering between localized exciton states is restricted to processes within the same valley, since intervalley scattering would involve at least two phonons. Phonon-driven scattering from a free to a localized state corresponds to a capture or an escape process.

Note that our system has to be in an orthogonal basis, i.e. it has to yield $\Phi_{qQ} = \chi_Q \phi_q$ where Φ_{qQ} are eigen vectors of an orthogonal system. To describe the continuum of states, we use plane waves and describe the free eigenfunctions by orthogonalized plane waves [4–6]:

$$|\phi^{OPW}_{Q}\rangle = \frac{1}{N_Q} \left(|\phi^{PW}_{Q}\rangle - \sum_{\mu m} \langle \chi^{\mu m}_{Q} | \phi^{PW}_{Q} \rangle | \chi^{\mu m}_{Q} \rangle \right) \tag{S5}$$

with the normalization factor $N_Q = \sqrt{1 - \sum_{\mu m} |\langle \chi^{\mu m}_{Q} | \phi^{PW}_{Q} \rangle|^2}$ and the plane waves ϕ^{PW}_{Q} which can be described in momentum space by a delta function around the Q_F, ie. $\phi^{PW}_{Q} \approx \delta_{Q,Q_F}$. Using this approach, we are able to calculate all scattering

and capture rates. We find that the capture of excitons is most likely to happen in the energetically closest localized state. Capture in energetically lower lying states appears on a much slower timescale and is hence negligible. The reason for that is the energy conservation in Eq. (S4). Furthermore, the relaxation dynamics within the localized states happen on a much faster time scale than capture processes, i.e. excitons decay almost immediately from any ns state to the lowest 1s state. Hence, it is most important to take into account the localized 1s states for the calculation of the optical response.

Assuming a Boltzman distribution for the free states $N^{\mu F}_{Q_F} \approx N^{\mu F}_0 e^{-\beta(E^{\mu F}_{Q_F}-E^{\mu F}_0)}$ yields to $\sum_{Q_F} N^{\mu F}_{Q_F} = N^{\mu F}_0 \kappa_\mu$ with $\kappa_\mu = \frac{M_\mu}{2\pi\hbar^2\beta}$ which enables us to evaluate Eq. (S1) and Eq. (S2). Taking all intra- and intervalley exciton-phonon scattering as well as capture and escape processes into account, we find for the dynamics of bright and momentum-dark exciton μ = KΛ,KK'), both free F and localized L states :

$$\dot{N}^{\mu F}_0 = \frac{1}{\kappa_\mu}\left[\Gamma^{\mu F,\text{form}} - \left(\Gamma^{\mu F,\text{rad}} + \Gamma^{\mu F\mu L\text{capt}}\right) N^{\mu F}_0 + \Gamma^{\mu L\mu F\text{esc}} N^{\mu L} + \sum_{\nu F}\left(\Gamma^{\mu F\nu F\text{in}} N^{\nu F}_0 - \Gamma^{\nu F\mu F\text{out}} N^{\mu F}_0\right)\right] \tag{S6}$$

$$\dot{N}^{\mu L} = \Gamma^{\mu L,\text{form}} - \left(\Gamma^{\mu L,\text{rad}} + \Gamma^{\mu L\mu F\text{esc}}\right) N^{\mu L} + \Gamma^{\mu F\mu L\text{capt}} N^{\mu F}_0 \tag{S7}$$

where we have introduced the radiative dephasing $\Gamma^{\mu F(L),\text{rad}}$ for the free (localized) state within the light cone, ie. μ=KK, a term $\Gamma^{\mu F(L),\text{form}} = \Gamma^{\mu F(L)\mu L}|P^{\mu L}|^2 + \sum_{\nu Q_F}\Gamma^{\mu F(L)\nu Q_F}|P^{\nu F}|^2$ which corresponds to the driving term due to decay of coherent excitons, $\Gamma^{\mu F\mu L\text{capt}} = \sum_{Q_F}\Gamma^{\mu F\mu L}_{Q_F} e^{-\beta E^{\mu F}_{Q_F}}$ as capture and $\Gamma^{\mu L\mu F\text{esc}} = \sum_{Q_F}\Gamma^{\mu L\mu F}_{Q_F}$ as escape rates, and finally for in and outscattering with phonons between free excitons $\Gamma^{\mu F\nu F\text{in}} = \sum_{Q_F Q'_F}\Gamma^{\nu F\mu F}_{Q'_F Q_F} e^{-\beta E^{\nu F}_{Q'_F}}$ and $\Gamma^{\mu F\nu F\text{out}} = \sum_{Q_F Q'_F}\Gamma^{\mu F\nu F}_{Q_F Q'_F} e^{-\beta E^{\mu F}_{Q_F}}$.

The radiative decay of both free and localized excitons is calculated by exploiting the corresponding wave functions obtained through the Wannier equation [7]. All appearing exciton-phonon scattering and capture/escape rates have been calculated on microscopic footing within the second-order Born-Markov approximation [8] and exploiting the orthogonalized plane wave approach [4–6] as discussed above. Solving Eq. (S6) provides access to time dependent exciton occupations in different exciton states entering the photoluminescence equation in the main manuscript.

LOCALIZED EXCITONS FOR A DEEPER DISORDER POTENTIAL

Here, we investigate localized excitons in analogy to the main text, however focusing now on a deeper disorder potential with $V_0 = 160$ meV reflecting well findings in recent photoluminescence excitation measurements [9]. As a result of the deeper potential, we find larger binding energies of localized excitons, cf. Fig. S1. Another consequence is that the phonon-induced capture processes are significantly weaker in particular with respect to the intervalley scattering. This leads to less pronounced features of localized excitons in PL spectra that are dominated by phonon-sidebands of momentum-dark excitons, cf. Fig. S2. Increasing the disorder width, the capture efficiency is enhanced due to larger overlaps of free and localized exciton wavefunctions and the increased role of higher localized excitonic states, cf. the inset in Fig. S3.

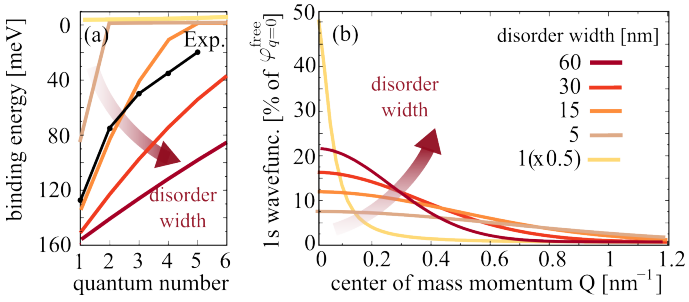

Figure S1. **Characteristics of localized excitons.** Disorder-width dependent (a) binding energies and (b) 1s wavefunctions of localized excitons. The calculated results are in good agreement with recent photoluminescence excitation measurements [9] (black line).

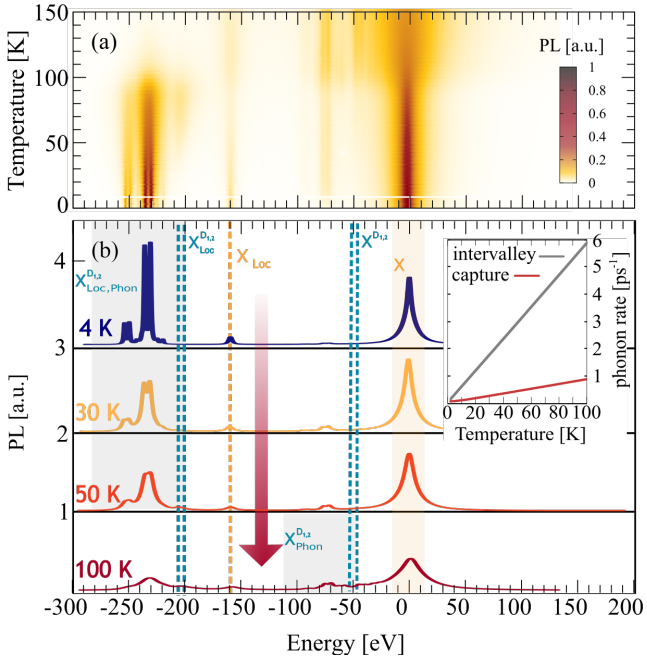

Figure S2. **Temperature dependent photoluminescence.** (a) Surface plot of time integrated photoluminescence for different temperatures and a fixed disorder potential with $\sigma = 30$ nm and $V_0 = 160$ meV. (b) 2D cuts from the surface plot at constant temperatures. Note that the spectra are shifted in energy so that the bright X exciton is located at 0 meV. The inset shows phonon-induced capture (red) and intervalley (gray) scattering rates.

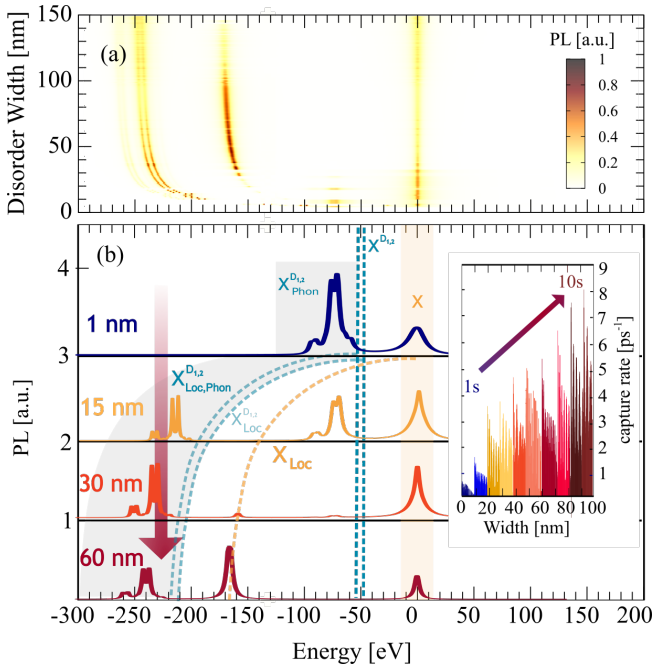

Figure S3. **Disorder-width dependent photoluminescence.** (a) Time-integrated photoluminescence spectra at 10 K for varying disorder width. (b) 2D cuts of the surface plot at four fixed widths. We predict clear signatures from both localized bright and dark excitons X_{Loc} and X^D_{Loc}. While for widths up to 50 nm phonon-assisted side bands from X^D_{Loc} are predominant, bright localized excitons X_{Loc} gain intensity for larger disorder widths reflecting the increasing capture rate, cf. the inset.

[1] M. Feierabend, G. Berghäuser, M. Selig, S. Brem, T. Shegai, S. Eigler, and E. Malic, Physical Review Materials **2**, 014004 (2018).
[2] M. Selig, G. Berghäuser, M. Richter, R. Bratschitsch, A. Knorr, and E. Malic, 2D Materials (2018).
[3] S. Brem, J. Zipfel, M. Selig, A. Raja, L. Waldecker, J. D. Ziegler, T. Taniguchi, K. Watanabe, A. Chernikov, and E. Malic, Nanoscale (2019).
[4] C. Herring, Physical Review **57**, 1169 (1940).
[5] H. Schneider, W. Chow, and S. W. Koch, physica status solidi (b) **238**, 589 (2003).
[6] E. Malić, K. J. Ahn, M. J. Bormann, P. Hövel, E. Schöll, A. Knorr, M. Kuntz, and D. Bimberg, Applied physics letters **89**, 101107 (2006).
[7] M. Selig, G. Berghäuser, A. Raja, P. Nagler, C. Schüller, T. F. Heinz, T. Korn, A. Chernikov, E. Malic, and A. Knorr, Nature communications **7**, 13279 (2016).
[8] D. F. Walls and G. J. Milburn, *Quantum optics* (Springer Science & Business Media, 2007).
[9] P. Tonndorf, R. Schmidt, R. Schneider, J. Kern, M. Buscema, G. A. Steele, A. Castellanos-Gomez, H. S. van der Zant, S. M. de Vasconcellos, and R. Bratschitsch, Optica **2**, 347 (2015).